In operando synchrotron X-ray radiography studies of polymer electrolyte membrane water electrolyzers

Michael A. Hoeh[1,*], Tobias Arlt[2] , Ingo Manke[2], John Banhart[2,3], David L. Fritz[1], Wiebke Maier[1], Werner Lehnert[1,4]

1) **Forschungszentrum Jülich GmbH, Institute of Energy and Climate Research, IEK-3: Electrochemical Process Engineering, 52425 Jülich, Germany**
2) **Helmholtz-Zentrum Berlin GmbH, Institute of Applied Materials, Hahn-Meitner-Platz 1, 14109 Berlin, Germany**
3) **Technische Universität Berlin, Hardenberg Str. 36, 10623 Berlin, Germany**
4) **Modeling in Electrochemical Process Engineering, RWTH Aachen University, Aachen, Germany**

* corresponding author. Tel.: +49 2461 61-9842; fax: +49 2461 61-6695. E-mail address: m.hoeh@fz-juelich.de

Abstract

Polymer electrolyte membrane water electrolyzers (PEL) are studied in-operando by synchrotron X-ray radiography. Two-phase flow phenomena associated with the evolution of oxygen and hydrogen in the surrounding water are investigated on a running electrolyzer cell. We examine the gas bubble discharge from the porous transport layer (PTL) into the flow channel and discuss the transport of bubbles in the flow channel. The transport of gas inside the PTL and the number of gas bubble discharge sites is examined and correlated with current density.

1. Introduction

Polymer electrolyte membrane water electrolysis (PEL) is increasingly attracting interest as a means to store electricity generated from intermittent renewable sources like wind or solar [1]. Electrolysis is currently considered one of the few available pathways to achieve a 100% renewable electricity supply [2]. PEL can accommodate higher current densities [1] and a wider range of operation compared to alkaline water electrolysis [3]. In PEL, water is typically supplied via flow channels and distributed across the catalyst layer through a porous transport layer (PTL). Gas evolution occurs at the catalyst layer, and the gas is transported back through the PTL and discharged into the flow channels, where it is transported out of the cell as a two-phase mixture with the feed water. For energy storage applications, higher current densities are desired [3], yet the resulting amount of gas produced could lower the overall cell performance due to mass transport restrictions induced by the reduced supply of water to the catalyst sites.

In the past, in-situ synchrotron X-ray radiography (SR) has been a valuable tool for visualizing processes inside operating electrochemical cells without substantial modification of cell layout or disruption of the electrochemical reactions. This method was first applied to running polymer electrolyte membrane fuel cells (PEFC) by Manke et al., which elucidated the formation and transport of liquid water for the verification of modelling approaches [4]. Further studies described the transport of water through the porous gas diffusion media [5] and eruptive water transport from the gas diffusion media to the flow channels [6]. SR was also applied to direct methanol fuel cells [7] and high-temperature PEFCs [8, 9].

Currently, only few studies have investigated two-phase flow phenomena in PEL. Dedigama et al. [10] examined the two-phase flow in the flow channel using a transparent window made of Perspex (Poly(methyl methacrylate or PMMA). Yet differences in contact angles and electrical conductivity of PMMA compared to typical flow channel materials like titanium [1] could introduce perturbations of the flow regime and disturb the current distribution within the cell. Selamet et al. combined neutron radiography with optical imaging to study the evolution of water thicknesses in a PEL cell over time [11]. However, the spatial resolution was limited to 15 µm for optical and 250 µm for neutron imaging. Selamet et al. also applied X-ray imaging to a regenerative fuel cell operated in the electrolysis mode using an X-ray microscope based on an X-ray tube, without reporting a spatial resolution [12].

On the contrary, spatial resolutions of <5 µm can easily be achieved with SR [13]. These resolutions are necessary to study the PTL of a running PEL cell, for which the mean pore diameter can be as low as 8 µm [14]. In this study, we report for the first time in-operando SR imaging of in-plane and through-plane two-phase flow inside a PEL.

2. Experimental

2.1 Cell preparation and design

Two PEL cells were used for the SR measurements, one with an active area of 11.9 cm^2 (#1) and one of 17.6 cm^2 (#2). Both cells utilize a Nafion N117 membrane (DuPont) coated with a cathode catalyst layer consisting of platinum on carbon (HISPEC 9100 with 60 wt.% Pt by Johnson Matthey) and Nafion (DuPont), and an anode catalyst layer containing iridium oxide (IrO_2 by Alfa Aesar) and Nafion (DuPont). On the anode side, a PTL composed of sintered titanium powder (GKN Sinter Metals) was employed while conventional Toray carbon paper (TGP-H-120 by Toray) directly obtained from Toray Industries (not treated with PTFE) was used on the cathode side. Graphite separator plates with a machined flow field structure were employed with either a meander-shaped single channel on anode and cathode (#1) or equally-spaced parallel channels on the cathode and a meander-shaped single channel on the anode (#2), as shown in figure 1. The channels were 1.4 mm wide and 0.4 mm deep.

The cells were operated at 80°C and ambient pressure. Both the anode side and the cathode side were continuously supplied with water. Water flow rates ranged from 0.6 to 1.5 ml/(min cm^2) while the current density was varied in the range of 10-200 mA/cm^2.

2.2 Synchrotron X-ray radiography

The radiographic measurements were performed at the synchrotron radiography station of the Helmholtz-Zentrum Berlin (BAMline at BESSY II). A monochromatic X-ray beam with an energy of 25 keV was chosen to ensure sufficiently high transmission through all cell components. An optical setup with a (4008 × 2672) $pixel^2$ CCD camera (PCO 4000 with a $CdWO_4$ scintillator screen) was used to capture images with a pixel size of 2.15 µm. The temporal resolution (including exposure time and readout time) was 5 s for the settings chosen.

3. Results & Discussion

The X-ray transmission images were normalized to preceding images. An increase in transmission (lighter area in the images) indicates an increase in the gas presence, as the X-ray attenuation coefficient of gases is orders of magnitude smaller than that of the surrounding liquid water. A decrease in transmission (darker area) indicates an increase of water in areas where gas was

previously present. These transmission variations allow for analyzing the transport of gas bubbles inside the cell.

In-plane SR was used to visualize gas bubble formation in an operating PEL cell at the PTL/flow channel interface. Figure 2a illustrates an image series taken on the cathode side interface at different times during the growth of a hydrogen bubble. Such growth proceeds until a critical diameter is reached at which the bubbles are discharged into the flow channel and new bubbles can be formed. The temporal evolution of the bubble diameter and the subsequent bubble discharge, at one specific location at the PTL/flow channel interface, is given in figure 2b for different current densities.

In the case of the discharge site shown in figure 2a, the average diameter at discharge, the periodicity of bubble formation and the moles n of gas ejected to the flow channel at the critical discharge diameter d are listed in Table 1 for current densities of 10, 75 and 200 mA/cm^2. n was calculated using the ideal gas law at atmospheric pressure p and gas volume given by the bubble diameter, assuming a spherical bubble,

$$n = \frac{p\left(\frac{4}{3}\pi\left(\frac{d}{2}\right)^3\right)}{RT} \qquad (1)$$

where R is the gas constant and T is the temperature. The gas production rate over the area A is linked to the current density j by Faraday's law

$$j = zF\frac{n}{At} \qquad (2)$$

where F is the Faraday constant, z is the number of electrons involved, and t is the time. In order to correlate the gas production at the catalyst layer with the gas ejection at the interface to the flow channel, a pore opening to the catalyst layer is considered. With a mean pore diameter of 31 µm for a Toray PTL [15], the area of this pore opening to the catalyst layer is obtained. From this area and the amount of gas ejected into the flow channel at the current densities of 10, 75 and 200 mA/cm^2, a hypothetical current density can be calculated (Table 1), which represents the current density that would be required at this pore opening to produce the amount of gas that is ejected to the flow channel at this discharge site as shown in figure 2a. It is found that these calculated hypothetical current densities decrease as the measured average current density increases (Table 1). This means that at lower current densities, more gas is ejected through fewer pores, potentially from sites around the pore opening on the catalyst layer. At higher current densities however, this implies that the gas produced must have been discharged through newly established pathways in the PTL. This can also be observed in figure 3a-d, where more discharge sites occur at higher current densities. Conversely, this means that the number of pathways for the discharge of gas and likewise the amount of water in the PTL, i.e. its saturation with water, is in general a function of current density. These results have important implications for modelling the two-phase flow inside the PTL of electrolyzer cells.

Through-plane measurements were performed where the X-ray transmission signal through the whole cell represents a superposition of the attenuation characteristics of each individual component (as depicted in figure 1). Hence, the gas/water flow in the anode and cathode channels are superimposed. The anode and cathode sides could be clearly separated, as the flow channel geometries were different, which allowed drawing conclusions on both sides of the cell individually. Figure 3e-g shows the gas transport in the anode and cathode channels. In the meander-shaped

anode channel spherical bubbles can be observed, while a larger slug is visible in the central cathode channel.

The amount of hydrogen in the cathode flow channel of the cell shown in figure 3a-d is shown in figure 4 at a current density of 10 mA/cm^2 and a water flow rate of 1.5 ml/(min cm^2). Within some 100 s after setting the operation point of the cell represented by figure 4, fluctuations in the transmission can be observed, indicating the passage of gas bubbles through the channel. A strong increase in transmission lasting for some 100 s can be seen after ~1200 s and again after ~1450 s. This reflects gas accumulation for a longer period at this position of the flow channel, indicating a temporarily immobile gas bubble pinned within the flow channels. This might be explained by the hydrophilicity of the graphite flow channel, which demonstrates that channel dimensions and wetting properties of the material used play a major role in facilitating the gas removal from the channel.

4. Summary

Two-phase flow phenomena in PEL cells were investigated in-operando by synchrotron X-ray radiography. The gas bubble discharge from the PTL into the flow channels was analyzed in terms of their frequency and the discharged gas volumes, suggesting the occurrence of selective transport pathways for the evolving gas in a water-saturated PTL. Furthermore, with increasing current density, more pathways for the gas transport are established and thus the water-saturation of the PTL depends directly on the current density. SR proves to be a valuable tool for elucidating two-phase flow phenomena and gaining insights into the gas-water distribution inside running PEL cells. The results obtained will benefit the modeling of two-phase flow in PEL cells, the design of cell components which facilitate gas removal and will contribute to a better understanding of mass transport restrictions in PEL.

Acknowledgements

The authors gratefully acknowledge Birgit Schumacher, Andreas Maintz, Daniel Holtz, Michael Hehemann and Stefanie Fischer (all Forschungszentrum Jülich), and Dr. Heinrich Riesemeier from the Federal Institute for Materials Research and Testing (BAM) for beam line support.

[1]
Carmo, M.; Fritz, D. L.; Mergel, J. & Stolten, D.
A comprehensive review on PEM water electrolysis
International Journal of Hydrogen Energy, **2013***, 38*, 4901 - 4934
http://dx.doi.org/10.1016/j.ijhydene.2013.01.151

[2]
Pleßmann, G.; Erdmann, M.; Hlusiak, M. & Breyer, C.
Global Energy Storage Demand for a 100% Renewable Electricity Supply
Energy Procedia , **2014***, 46*, 22 - 31
http://dx.doi.org/10.1016/j.egypro.2014.01.154

[3]
Ursua, A.; Gandia, L. & Sanchis, P.
Hydrogen Production From Water Electrolysis: Current Status and Future Trends
Proceedings of the IEEE, **2012***, 100*, 410-426
http://dx.doi.org/10.1109/JPROC.2011.2156750

[4]
Manke, I.; Hartnig, C.; Grünerbel, M.; Lehnert, W.; Kardjilov, N.; Haibel, A.; Hilger, A.; Banhart, J. & Riesemeier, H.
Investigation of water evolution and transport in fuel cells with high resolution synchrotron x-ray radiography
Applied Physics Letters, AIP, **2007***, 90*, 174105
http://dx.doi.org/10.1063/1.2731440

[5]
Hartnig, C.; Manke, I.; Kuhn, R.; Kardjilov, N.; Banhart, J. & Lehnert, W.
Cross-sectional insight in the water evolution and transport in polymer electrolyte fuel cells
Applied Physics Letters, AIP, **2008***, 92*, 134106
http://dx.doi.org/10.1063/1.2907485

[6]
Hartnig, C.; Manke, I.; Kuhn, R.; Kleinau, S.; Goebbels, J. & Banhart, J.
High-resolution in-plane investigation of the water evolution and transport in PEM fuel cells
Journal of Power Sources , **2009***, 188*, 468 - 474
http://dx.doi.org/10.1016/j.jpowsour.2008.12.023

[7]
Hartnig, C.; Manke, I.; Schloesser, J.; Krüger, P.; Kuhn, R.; Riesemeier, H.; Wippermann, K. & Banhart, J.
High resolution synchrotron X-ray investigation of carbon dioxide evolution in operating direct methanol fuel cells
Electrochemistry Communications, **2009***, 11*, 1559 - 1562
http://dx.doi.org/10.1016/j.elecom.2009.05.047

[8]
Maier, W.; Arlt, T.; Wannek, C.; Manke, I.; Riesemeier, H.; Krüger, P.; Scholta, J.; Lehnert, W.; Banhart, J. & Stolten, D.
In-situ synchrotron X-ray radiography on high temperature polymer electrolyte fuel cells

Electrochemistry Communications, **2010***, 12*, 1436 - 1438
http://dx.doi.org/10.1016/j.elecom.2010.08.002

[9]
Arlt, T.; Maier, W.; Tötzke, C.; Wannek, C.; Markötter, H.; Wieder, F.; Banhart, J.; Lehnert, W. & Manke, I.
Synchrotron X-ray radioscopic in situ study of high-temperature polymer electrolyte fuel cells - Effect of operation conditions on structure of membrane
Journal of Power Sources , **2014***, 246*, 290 - 298
http://dx.doi.org/10.1016/j.jpowsour.2013.07.094

[10]
Dedigama, I.; Angeli, P.; Ayers, K.; Robinson, J.; Shearing, P.; Tsaoulidis, D. & Brett, D.
In situ diagnostic techniques for characterisation of polymer electrolyte membrane water electrolysers – Flow visualisation and electrochemical impedance spectroscopy
International Journal of Hydrogen Energy, **2014***, 39*, 4468 - 4482
http://dx.doi.org/10.1016/j.ijhydene.2014.01.026

[11]
Selamet, O.; Pasaogullari, U.; Spernjak, D.; Hussey, D.; Jacobson, D. & Mat, M.
Two-phase flow in a proton exchange membrane electrolyzer visualized in situ by simultaneous neutron radiography and optical imaging
International Journal of Hydrogen Energy , **2013***, 38*, 5823 - 5835
http://dx.doi.org/10.1016/j.ijhydene.2013.02.087

[12]
Selamet, O. F.; Deevanhxay, P.; Tsushima, S. & Hirai, S.
Visualization of Gas Bubble Behavior of a Regenerative Fuel Cell in Electrolysis Mode by Soft X-ray Radiography
ECS Transactions, **2013***, 58*, 353-360
http://dx.doi.org/10.1149/05801.0353ecst

[13]
Schröder, A.; Wippermann, K.; Arlt, T.; Sanders, T.; Baumhöfer, T.; Markötter, H.; Mergel, J.; Lehnert, W.; Stolten, D.; Manke, I. & Banhart, J.
Water Evolution in Direct Methanol Fuel Cell Cathodes Studied by Synchrotron X-Ray Radiography
Fuel Cells, WILEY-VCH Verlag, **2013***, 13*, 371-379
http://dx.doi.org/10.1002/fuce.201300041

[14]
Grigoriev, S.; Millet, P.; Volobuev, S. & Fateev, V.
Optimization of porous current collectors for PEM water electrolysers
International Journal of Hydrogen Energy, 2009, 34, 4968 - 4973
http://dx.doi.org/10.1016/j.ijhydene.2008.11.056

[15]
Odaya, S.; Phillips, R.; Sharma, Y.; Bellerive, J.; Phillion, A. & Hoorfar, M.
X-ray Tomographic Analysis of Porosity Distributions in Gas Diffusion Layers of Proton Exchange Membrane Fuel Cells
Electrochimica Acta , 2015, 152, 464 – 472
http://dx.doi.org/10.1016/j.electacta.2014.11.143

Measured average current density [mA/cm^2]	Average diameter at discharge [µm]	Bubble formation periodicity [s]	Ejected gas amount [mol/s]	Hypothetical current density [mA/cm^2]
10	73 ± 7	60 ± 6	6.6×10^{-12}	168
75	61 ± 8	45 ± 6	5.1×10^{-12}	129
200	51 ± 13	23 ± 6	5.9×10^{-12}	151

Tab. 1: Discharge diameters and bubble formation periodicity as obtained from fig. 2. Gas amount and hypothetical current density were calculated as discussed in section 3.

Fig. 1 (a) Sketch of the PEL cell showing the components separator plates, titanium PTL, MEA, carbon PTL with indication of beam direction for in-plane and through-plane measurements. (b) Flow field structures used for in-plane and through-plane.

Fig. 2 (a) Visualization of the growth of a hydrogen bubble at the interface between PTL and cathode flow channel to the critical diameter at which the bubble is discharged into the cathode flow channel (t=50s) and a new bubble is formed (t=60s). Cell operated at 10 mA/cm^2 at a flow rate of 1.5 ml/(min cm^2), in-plane view. Water stream from bottom to top. (b)-(d) Evolution of the diameter of this single hydrogen bubble at current densities b 10 mA/cm^2, c 75 mA/cm^2, and d 200 mA/cm^2.

Fig. 3 (a)-(d) Visualization of the increase in number of discharge sites at two locations along the PTL-cathode channel interface at 10 mA/cm^2 (a, c) and 200 mA/cm^2 (steady-state) (b, d), at a flow rate of 1.5 ml/(min cm^2), (e)-(g) visualization of gas transport in the anode (solid line) and cathode channels (dashed line) at 200 mA/cm^2, through-plane view. Water flow rate 0.6 ml/(min cm^2), from bottom to top. A larger slug can be observed in the central cathode channel (white arrow), bubbles are visible in the anode channel.

Fig. 4: Evolution of hydrogen volume in one cathode flow channel. Cell operated at 10 mA/cm^2. Data derived from experiment shown in fig. 3(e), but a different area of the cell was selected for analysis.

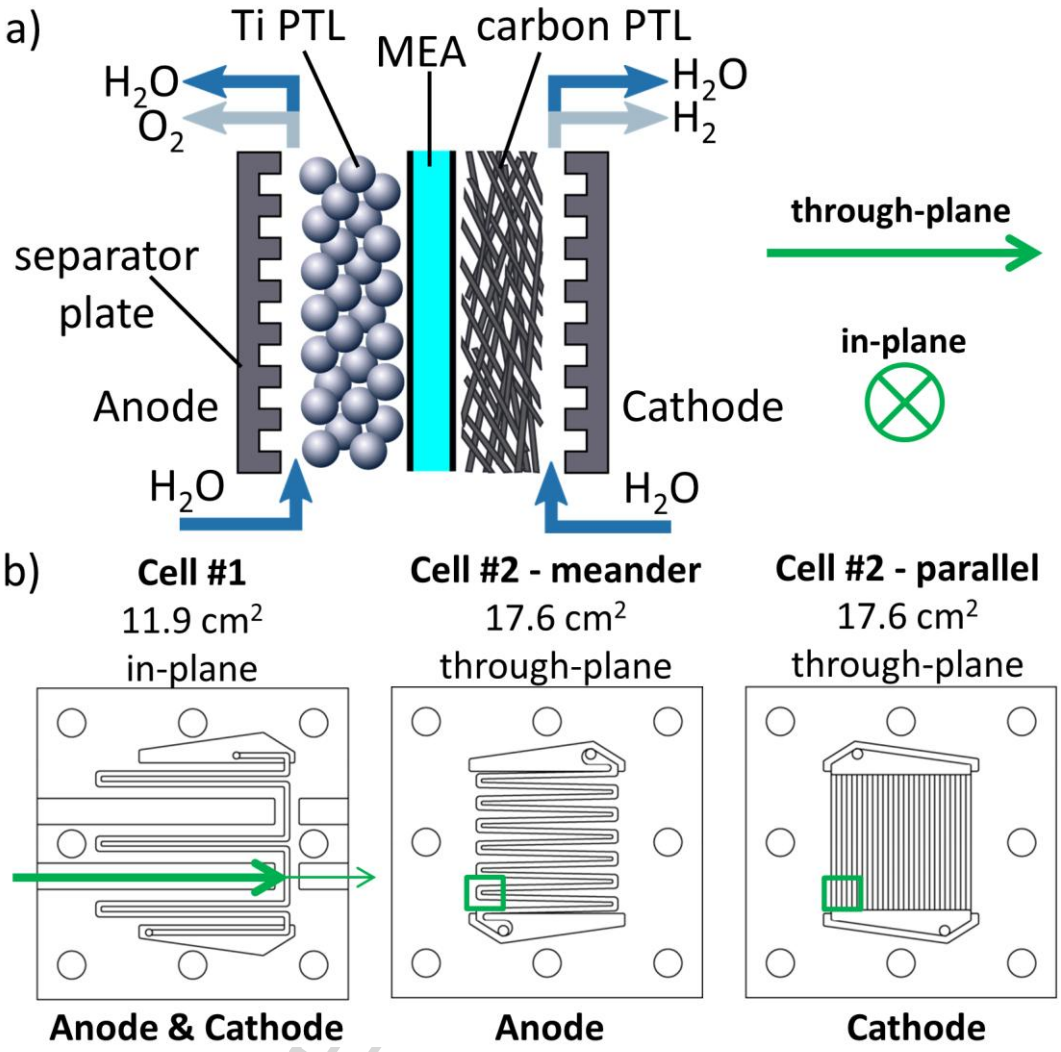

Figure 1

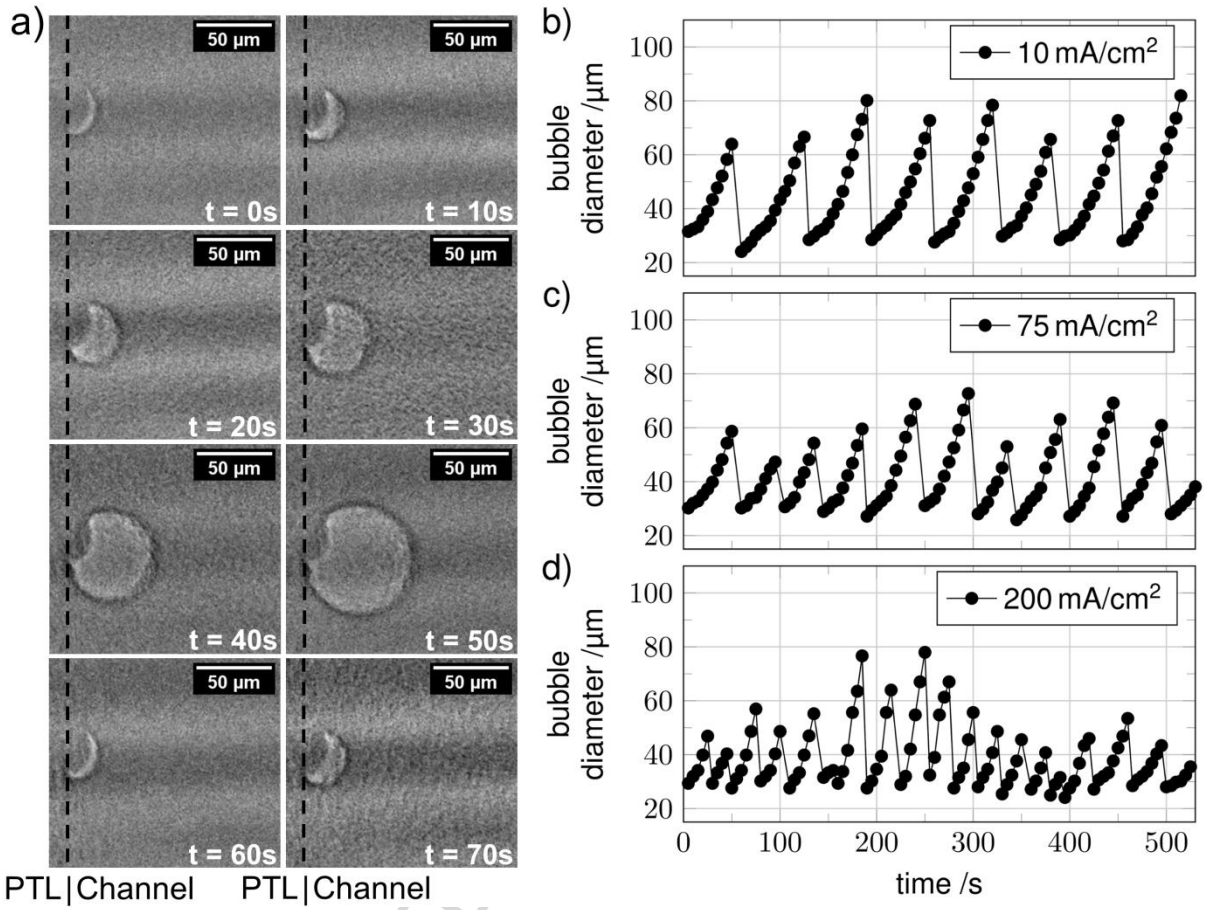

Figure 2

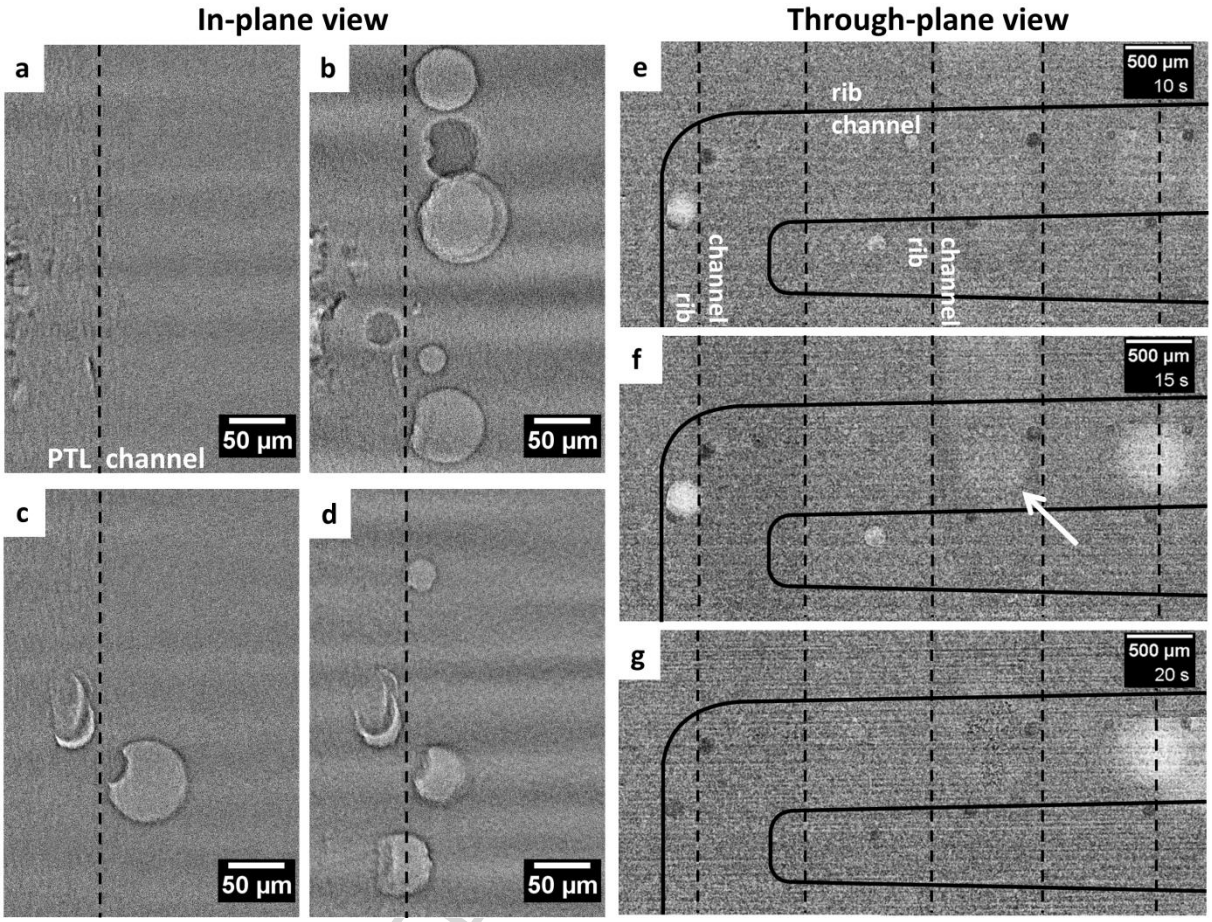

Figure 3

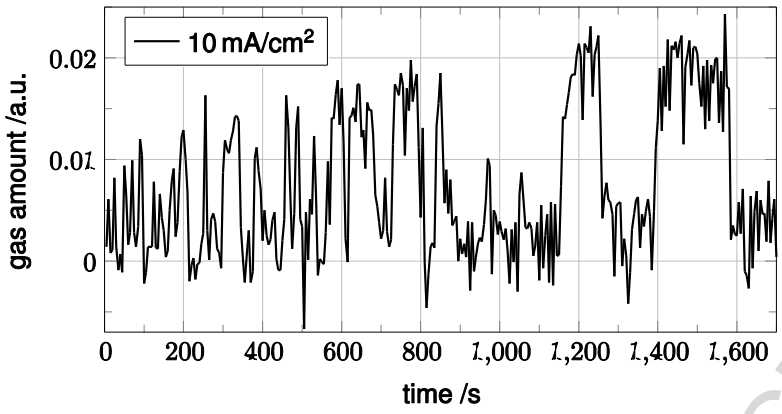

Figure 4

Highlights

- Synchrotron X-ray radiography was applied to polymer electrolyte membrane water electrolyzers.
- Gas transport in the porous transport layer occurs through selective pathways.
- The number of pathways for the gas transport are a function of current density.